

# Modeling and Fitness Landscape Analysis for Flexible MBMS Radio Resource Allocation

Qing Xu\*, Frédéric Lassabe<sup>§</sup>, Mabed Hakim\* and Alexandre Caminada \*

\* IRTES-SeT, Université de Technologie de Belfort-Montbéliard, France

Email: (qing.xu, frederic.lassabe, alexandre.caminada)@utbm.fr

<sup>§</sup> Département d'Informatique des Systèmes Complexes(FEMTO-ST)

Université de Franche-Comté, France

Email: hakim.mabed@pu-pm.univ-fcomte.fr

**Abstract**—The Multimedia Broadcast Multicast Service (MBMS) system supports efficient diffusion of multicast multimedia services in cellular networks. We develop a flexible model to perform dynamic radio resource allocation for MBMS service by using metaheuristic approach. We conduct fitness landscape analysis to study the characteristics of the proposed problem, which helps us to select appropriate search strategies. Simulation results show that the proposed algorithm provides better performance than existing algorithms.

**Index Terms**—modeling; fitness landscape analysis; multimedia multicast service; radio resource management

## I. INTRODUCTION

The MBMS system [6] specified by the 3GPP is considered as a substantial and efficient platform for multicast service over cellular networks. The MBMS service over UMTS Terrestrial Radio Access Network (UTRAN) interfaces could be carried by PTM (point-to-multipoint) and PTP (point-to-point) mode. In PTM mode, service is carried by a Forward Access Channel (FACH) covering the whole cell. Each FACH needs one channel code serving large amount of users, but may waste power when users are very close to the base station [7]. The PTP mode uses Dedicated Transport Channel (DCH) or High-Speed Downlink Shared Channel (HS-DSCH). Each DCH needs one channel code serving one dedicated user and the shared channel occupies up to 15 channel codes for users. PTP mode provides better link quality than PTM mode but the served user number is limited due to power and channel code restrictions [5]. In UTRAN where the radio resources (power and channelization codes) are limited, the selection of transmission mode is crucial for the allocation efficiency. The related work on this topic are:

**MBMS Power Counting** (MPC) proposed to establish PTP connections for one MBMS service when the estimated power consumption is under an operator-defined threshold [5]. The switch from PTP to PTM occurs when power exceeds the threshold, and vice versa. MPC is easy to implement but it has limited flexibility because it only considers the delivery of service for all users with the same service quality.

**Dual transmission mode** (DTM) allows the co-existing usage of PTP and PTM mode for one MBMS service [8]. FACH coverage is adapted for the users who are close to the base station, meanwhile the DCH connections are released

or established for the users near the cell edge. However, simulation concludes that DTM is only beneficial for up to 5 users [2]. Hence it is rather limited by only applying FACH and DCH for co-existing of transmission modes.

**Scalable FACH Transmission** (S-FACH) saves transmission power for MBMS service by integrating scalable video coding technology [9]. The scalable encoded service can be divided into single layer (SL) and multiple layer (ML) transmission schemes. ML service can be splitted into several flows with lower bit rate hence with lower QoS requirement compared with a non-scalable stream. (e.g. 256 kbps service is splitted into two 128 kbps flows). S-FACH transmits flows through common channels with predefined coverage [9]. The basic flow is sent to all subscribers to guarantee service reception, the advanced flow is sent within 50% coverage to enhances service quality on top of basic layer. The trade-off can be made between QoS and the transmission power consumption. However, S-FACH is still based on the fixed coverage so that the resource allocation can not be optimal.

One key feature of radio resource allocation problem in the mobile environment is that the user scenario can be quite dynamic and flexible: the user number, user distributions and service requests can be quite different from time to time. The above existing approaches, however, has the limited flexibility such that the solution space can not be deeply explored. To address this problem, we propose a Flexible Radio Resource Management Model (F2R2M) and we aim to explore the solution space by using metaheuristic approach over the proposed model. In the proposed model, two neighborhood operators and a lexicographic-order criterion are proposed to evaluate the solution quality. Moreover, to understand the structure of solution space and the neighborhood space, we conduct the fitness landscape analysis of two neighborhood functions for different scenarios. The operation selection is further discussed and verified by simulations.

This paper is structured as follows. The proposed model is formulated in section II. Fitness landscape analysis of the model are discussed in section III. The simulation result is showed in section IV and section V is the conclusion and perspective.

## II. MODEL DESCRIPTION

This section describes the proposed model, which allows flexible resource allocation for scalable encoded multimedia multicast service.

### A. A Three-Phase Model

As shown in Figure 1, F2R2M is implemented in each radio network controller (RNC), performing radio resource allocation for simultaneous multicast service in the same cell through three phases. A cell is the coverage of one base station.

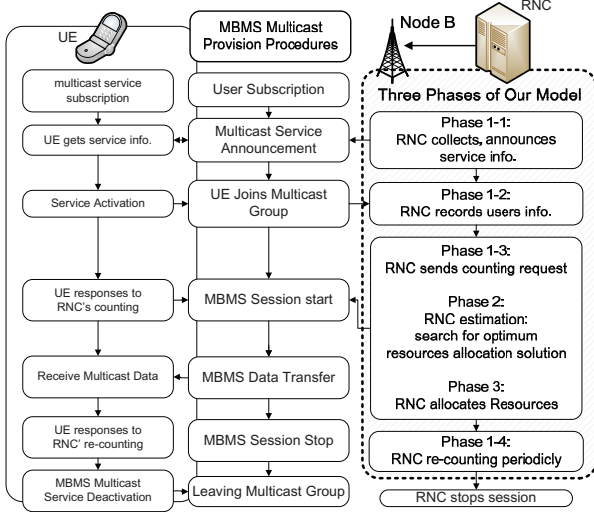


Fig. 1. Three phases of F2R2M

In the first phase (the collect phase), RNC periodically collects service and user information. Any change of MBMS session state (e.g. user mobility, new MBMS session) will trigger the second phase (the estimation phase) to search for proper allocation scheme. After that, according to the solution obtained in the previous phase, the third phase (the allocation phase) establishes the transmission power and channel codes allocation for selected users.

In the collect phase, RNC receives following variables as the input of model:

- $T(c) = \{t_1, \dots, t_{N_t}\}$ , a set of users located in cell  $c$ .
- $C(c) = \{(x_1, y_1), \dots, (x_{N_t}, y_{N_t})\}$ , the instantaneous geometry coordinates of  $T(c)$ .
- $S(c) = \{s_1, \dots, s_{N_s}\}$ , A set of services is going to be transmitted to multicast groups within  $c$ .
- $F(s_i) = \{f_{s_i,1}, f_{s_i,2}, f_{s_i,3}\}$  or  $\{f_{s_i,0}\}$ , the flows (and their bandwidth) of service  $s_i$ .  $f_{s_i,0}$  indicates  $s_i$  is SL transmission, and  $f_{s_i,j}$  ( $j > 0$ ) is the sublayer of ML scheme service.
- $Dist(s_i) = \{t_n, t_m, \dots\}$ ,  $s_i \in S(c)$ , the multicast group of  $s_i$  is constructed by users in  $T(c)$ .

F2R2M allows the flexible allocation of PTM and PTP modes for each flow, hence the possible assignment of transport channel include:

- pure PTM mode: only FACH,

- pure PTP mode: DCH or HS-DSCH,
- mix of PTP mode: DCH and HS-DSCH transfer the same flow content to different users,
- mix of PTP and PTM mode: co-existing of FACH, DCH or/and HS-DSCH.

Therefore, for each flow  $f_{s,j}$  of service  $s$ , we partition the multicast group  $Dist(s)$  into four disjointed sets:  $UE_{fach}(f_{s,j})$ : users served through a FACH;  $UE_{dch}(f_{s,j})$ : users transferred through DCHs;  $UE_{hs}(f_{s,j})$ : users sharing HS-DSCH and  $UE_{noch}(f_{s,j})$  includes non-served users.

The user partition is firstly determined in solution initialization, and to be modified in each iteration of optimization procedure. We define  $Rt(f_{s,j})$  to represent the users who are receiving  $f_{s,j}$ :  $Rt(f_{s,j}) = UE_{fach}(f_{s,j}) \cup UE_{dch}(f_{s,j}) \cup UE_{hs}(f_{s,j})$ . The decision of user sets follow two principles:

- 1)  $Rt(f_{s,j}) = Dist(s), j = 0, 1,$
- 2)  $Rt(f_{s,j}) \subseteq Rt(f_{s,j-1}), j \geq 2.$

The principle 1 is to guarantee the service coverage, which means all users in multicast group should be selected to receive  $f_{s,0}$  or  $f_{s,1}$ . The principle 2 restricts that the advanced flow is only sent to users who also receive lower flow, that is to avoid the redundant content transfer to the same user.

The user partition for  $f_{s,j}$  should be in accord with channel characteristics:

- 1)  $d_{t_i} \leq d_{thr}, \forall t_i \in UE_{fach},$
- 2)  $d_{t_j} > d_{thr}, \forall t_j \in UE_{dch} \cup UE_{hs} \cup UE_{noch},$
- 3)  $UE_{ch_m} \cap UE_{ch_n} = \phi, ch_m, ch_n \in \{fach, dch, hs, noch\}.$

In these constraints,  $d_{t_i}$  is the distance of user  $t_i$  from the base station.  $d_{thr}$  is the distance threshold determined during optimization procedure. FACH is a common channel and can be listened by all users within its coverage, the constraint 1 is to guarantee that  $UE_{fach}(f_{s,j})$  includes the nearest users in multicast group. is determined during optimization procedure. In the constraint 2, the users in multicast group, farther than the FACH coverage, are assigned to HS-DSCH or DCH. When there is no available channel code for a given users, this user is switched to  $UE_{noch}(f_{s,j})$ . Constraint 3 guarantees that user sets for each flow does not overlap. Since sending the same flow to user through more than one channel will waste resource.

Consequently, according to  $UE_{type}(f_{s,j})$  and requested flows bandwidth, available channel codes(s) is associated with a nonempty user set. This allocation procedure corresponding to the orthogonal principle of OVFSF (Orthogonal variable spreading factor) codes [1], if one code on the OVFSF tree is used, all codes underneath it are no longer usable.

When user and channel code allocation are determined, the power consumption of transport channels is implicitly determined. As shown in Figure 2, the downlink transmission power of FACH depends on its cell coverage [3], i.e.the user distribution in  $UE_{fach}(f_{s,j})$ .

The total transmission power of DCH for  $n$  users in a cell [13] is calculated by Equation 1:

$$P_{DCHs} = \frac{P_p + \sum_{i=1}^n L_{p,i} \cdot \frac{P_p + x_i}{(E_b/N_o)R_{b,i} + p}}{1 - \sum_{i=1}^n \frac{p}{(E_b/N_o)R_{b,i}} + p} \quad (1)$$

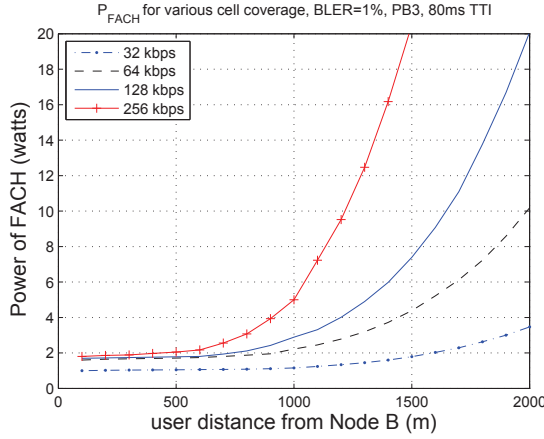


Fig. 2. Power of FACH [3]

where  $P_p$  is common channel power,  $P_n$  is the background noise,  $L_{p,i}$  is path loss of  $i$ th user,  $W$  is the bandwidth in UMTS,  $R_{b,i}$  is user transmit rate,  $E_b/N_o$  is the target experienced signal quality of user,  $p$  the orthogonality factor ( $p = 0$  represents perfect orthogonality).  $x_i$  is the intercell interference observed by  $i$ th user, expressed by  $x_i = \sum_{j=1}^M \frac{P_{Tj}}{L_{ij}}$ ,  $P_{Tj}$  is the transmission power in neighbor cell  $c_j$  ( $j = 1 \dots M$ ),  $L_{ij}$  is the path loss from  $i$ th user to  $j$ th cell.

The transmit power to guarantee a required HS-DSCH throughput [12] is expressed as:

$$P_{\text{HS-DSCH}} \geq \text{SINR} \times [p - G^{-1}] \frac{P_{\text{own}}}{SF_{16}} \quad (2)$$

in which  $P_{\text{own}}$  is the own cell interference experienced by user,  $G$  is the geometry factor defined by  $G = \frac{P_{\text{own}}}{P_{\text{other}} + P_{\text{noise}}}$ , related with the user position. For a user at the cell edge, The interference from the neighboring cells for is higher than the interference at its own cell, thus  $G$  is expressed by a lower value. In the macrocell (hexagonal layout with 1000 m base station spacing), users within 80% coverage experience a geometry factor of  $-2.5\text{dB}$  or better, within 95% a geometry factor at least  $-5.2\text{dB}$  [10]. With the target BLER and the channel quality information (CQI) from users, we obtain the Signal to Interference Noise Ratio (SINR) by applying the CQI and target BLER (i.e. 1%) from the analytic formulation driven by link-level simulation results in [11]. The CQI is obtained through the target bandwidth and mapping table of MAC-hs Bit Rates versus CQI [4]. Then  $P_{\text{hs}}$  is calculated by applying SINR and  $G$  into equation  $P_{\text{HS-DSCH}}$ .

### B. Fitness Values and Evaluation Criteria

The optimization target of F2R2M is first to guarantee the QoS requirement, then to minimize the transmission power while avoiding power saturation. The solution fitness is defined to reflect these aspects. The first objective is to minimize the loss of throughput in one cell:

$$\text{Th}(x) = \sum_{s_i \in S(c)} \sum_{f_j \in F(s_i)} \sum_{t_u \in \text{Dist}(s_i)} \max[-\Delta_{j,u}, 0] \quad (3)$$

subject to:  $SF_m(f_{s_i,j}) \perp SF_n(f_{s_i,j}), f_{s_i,j} \in F(s_i)$

The constraint guarantees the OVFS code orthogonality: channel codes are chosen to be orthogonal to each other in the same cell.  $\Delta_{j,u}$  in Equation 3 is the difference between allocated channel bit rate (determined by its OVFS code(s) [1]) and the flow bandwidth. For example, user  $t_u$  receives  $f_{s,j}$  (64 kbps) through DCH channel with bandwidth 32 kbps (SF = 64), then  $-\Delta_{j,u}$  is:  $-(32 - 64) = 32$  kbps.

The second optimization objective is to minimize the power consumption of cell:

$$Po(x) = \sum_{s_i \in S(c)} \sum_{f_j \in F(s_i)} \sum_{ch_l} P(f_{s_i,j}, ch_l), ch_l \in \{\text{fach}, \text{dch}, \text{hs}\}$$

meanwhile,  $Po(x) \leq P_{\text{MBMS\_budget}}(c)$ , which enforces the total power consumption of one cell to simultaneous MBMS services does not beyond the maximum power budget.

With the two-dimensional fitness value, the comparison of a new solution  $x'$  and current solution  $x$  is conducted in lexicographic order:  $x'$  is evaluated as better solution when  $\text{Th}(x') = \text{Th}(x)$  and  $Po(x') \leq Po(x)$ , or  $\text{Th}(x') < \text{Th}(x)$ .

### C. Solution Representations and Distance Measurement

To analyze the relationship between solutions and landscape, the distance between two feasible solutions need to be developed. We propose two solution representations and corresponding distance measurement.

1) *Representation A*: In the first representation, the solution of one cell is represented as a matrix of  $Nt$  rows and  $Nf$  columns:

$$x = \begin{pmatrix} f(s_1, 1) & f(s_1, 2) & \dots & f(s_{Ns}, 0) \\ ch_{1,1} & ch_{1,2} & \dots & ch_{1,Nf} \\ \dots & \dots & \dots & \dots \\ ch_{i,1} & ch_{i,2} & \dots & ch_{i,Nf} \\ ch_{j,1} & ch_{j,2} & \dots & ch_{j,Nf} \\ \dots & \dots & \dots & \dots \\ ch_{Nt,1} & ch_{Nt,2} & \dots & ch_{Nt,Nf} \end{pmatrix},$$

$$d(t_i) \leq d(t_j), i < j; ch_{i,j} \in \{-1, 0, 1, 2, 3\}$$

$Nf$  is the number of flows of all services in cell.  $Nt$  is the number of all users in cell.  $x(i, j)$  indicates the channel allocation of user  $t_i$  for flow  $f_j$ . Values 0, 1, 2, 3 represent user is allocated to UE(noeh, fach, dch, hs), -1 means the user does not belong to the multicast group.

Hamming distance is a well-known distance in combinatorial optimization, it corresponds to the number of different elements between two solutions. For solution representation A, we use hamming distance  $d_{\text{Ham}}$  to measure the distance between two feasible solutions represented by method A.

2) *Representation B*: In the second mathematical representation, the solution of flow  $f_{s,j}$  is a vector of users:

$$x(f_{s,j}) = \underbrace{(0, 1, 2, \dots, 0, i, \dots, 0, j, \dots, 0, k, \dots, t_{Nt})}_{\text{UE(fach)} \quad \text{UE(dch)} \quad \text{UE(hs)} \quad \text{UE(noeh)}}$$

The four user sets are separated by 0 and listed in fixed order. In each set itself, users are ordered with increased distance from the base station. Then the solution representation B of cell  $c$  is a vector consisting solutions of transmitted flows:

$$x(c) = \{x(s_1), \dots, x(s_{N_s})\} \\ = \{\dots, x(f_{s_i,0}), [x(f_{s_i,1}), x(f_{s_i,2}), \dots], \dots\}, \forall s_i \in S(c)$$

3) *Comparative Distance*: For solution representation B, we design the distance with structural comparisons, named comparative distance  $d_{com}$ . Assume we have two solutions based on representation B:  $x_B$  and  $x'_B$ . For the solution of same flow in  $x_B$  and  $x'_B$ , we count the number of users that are allocated to different channels, then the number of counted users is then marked as  $d_{Com}$ .

The comparative algorithm measures the exact minimum number of applications based on insert operator. It could also be utilized to measure the approximate distance of solutions generated by hybrid-moves operator.  $d_{Com}$  is essential the same value as  $d_{Ham}$ , the latter compares the different allocated values for all users in cell. Solution representation B as well as the comparative distance only include the users within multicast group for each flow, hence requiring less memory cost, we use the solution representation B and the comparative distance for following analysis.

#### D. Neighborhood Operators

At each iteration, a move is made to transform each solution into a neighbor solution. Based on the channel characteristic and solution representation, we define two neighborhood operators.

1) *Hybrid-moves operator*: The ‘‘Hybrid-moves’’ operator  $\delta_H$  is implemented in three steps: 1) choose one channel  $ch_o$ , with non-empty user allocation,  $UE_{ch_o}$  is a ‘‘output’’ set; 2) select another user set  $UE_{ch_i}$  as an ‘‘input’’ set ( $ch_i \neq ch_o$ ); 3) randomly select user  $t_k$  from  $UE_{ch_o}$ ,  $\delta_H$  moves this single  $t_k$  or a block of users including  $t_k$  from  $UE_{ch_o}$  to  $UE_{ch_i}$ . In the third step, the moved users depends on the chosen  $ch_i$  and  $ch_o$ . For example, once we decide to move  $t_k$  from  $UE_{hs}$  to  $UE_{fach}$ , we will enlarge the FACH coverage to  $t_k$ , in that case, all the users that nearer than  $t_k$  can now hear from FACH, thus, no matter what user sets they are currently allocated at, they need to stay or be inserted in FACH user set. Therefore, once we choose a user  $t_k$  to be moved to FACH set, we need to first check the user distributions served by the other channels, and pick out the users within the enlarged FACH coverage to  $UE_{fach}$ . By contraries, once we decide to move users out of  $UE_{fach}$ , i.e. reduce the FACH coverage, in that case, all users farther than  $t_k$  within  $UE_{fach}$  should be picked out and moved to the chosen  $ch_i$ .

In the following example, two steps of hybrid-moves operator are conducted, moving  $x_{h1}$  to  $x_{h2}$  then to  $x_{h3}$ :

$$x_{h1} : (0 \ 1 \ \underline{2} \ \underline{12} \ 0 \ 4 \ 5 \ 7 \ 8 \ 0 \ 6 \ 9 \ 0 \ 10 \ 11) \\ x_{h2} : (0 \ 1 \ 0 \ \underline{2} \ \underline{12} \ 4 \ 5 \ 7 \ 8 \ 0 \ \underline{6} \ 9 \ 0 \ 10 \ 11) \\ x_{h3} : (0 \ 1 \ 0 \ 2 \ 12 \ 4 \ 5 \ \underline{6} \ 7 \ 8 \ 0 \ 9 \ 0 \ 10 \ 11)$$

- $x_{h1} \rightarrow x_{h2}$ :  $ch_o = \text{FACH}$ ,  $ch_i = \text{DCH}$ ,  $t_k = t_2$ . FACH coverage is reduced. Both  $t_2$  and  $t_{12}$  are moved to DCH user set, because  $t_{12}$  is farther than  $t_2$ .
- $x_{h2} \rightarrow x_{h3}$ :  $ch_o = \text{HS-DSCH}$ ,  $ch_i = \text{DCH}$ ,  $t_k = t_6$ .

2) *Insert Operator*: The insert operator  $\delta_I$  moves only one user for each operator application. When FACH is chosen as  $ch_i$  or  $ch_o$ ,  $t_k$  is determinately selected: the nearest user within  $UE_{hs} \cup UE_{dch} \cup UE_{noch}$ , or the farthest user within  $UE_{fach}$ .

Consider  $x_{h1}$  and  $x_{h3}$  in previous example, three steps of insert operator are needed:

$$x_{i1}(x_{h1}) : (0 \ 1 \ 2 \ \underline{12} \ 0 \ 4 \ 5 \ 7 \ 8 \ 0 \ 6 \ 9 \ 0 \ 10 \ 11) \\ x_{i2} : (0 \ 1 \ \underline{2} \ 0 \ \underline{12} \ 4 \ 5 \ 7 \ 8 \ 0 \ 6 \ 9 \ 0 \ 10 \ 11) \\ x_{i3}(x_{h2}) : (0 \ 1 \ 0 \ \underline{2} \ \underline{12} \ 4 \ 5 \ 7 \ 8 \ 0 \ \underline{6} \ 9 \ 0 \ 10 \ 11) \\ x_{i4}(x_{h3}) : (0 \ 1 \ 0 \ 2 \ 12 \ 4 \ 5 \ \underline{6} \ 7 \ 8 \ 0 \ 9 \ 0 \ 10 \ 11)$$

- $x_{i1} \rightarrow x_{i2}$ :  $ch_o = \text{FACH}$ ,  $ch_i = \text{DCH}$ , the farthest user  $t_{12}$  in  $UE_{fach}$  is moved to  $UE_{dch}$ .
- $x_{i2} \rightarrow x_{i3}$ :  $ch_o = \text{FACH}$ ,  $ch_i = \text{DCH}$ ,  $t_2$  is determined.
- $x_{i3} \rightarrow x_{i4}$ :  $ch_o = \text{HS-DSCH}$ ,  $ch_i = \text{DCH}$ ,  $t_6$  is selected.

### III. FITNESS LANDSCAPE ANALYSIS

Fitness landscape was originally proposed in a study of evolutionary theory [15]. This notion was then applied to characterize a combinatorial optimization problem [14]. In order to get insight into the given problem, we conduct fitness landscape analysis on the proposed model.

We designed six scenarios with different service parameter settings and user distributions as in Figure 3. Each subfigure presents two scenarios with the same multicast groups and traffic load, but service  $s_2$  is transmitted as one 128 kbps flow in one of the two scenarios, while in another scenario it is transmitted as two flows at 64 kbps.

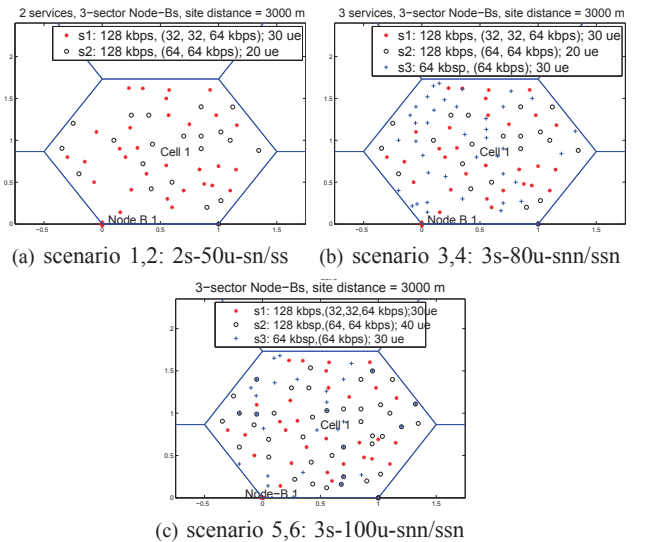


Fig. 3. User Distribution of Simulation Scenarios

The simulation parameters are listed in Table I. Consider one cell in a hexagonal structure of 19 cells, only multicast

services are transmitted in this cell. The maximum power for MBMS in one cell is 19 w (total transmission power minus the power for common channel).

TABLE I  
PARAMETER SETTING

Parameters	Value	Parameters	Value
Base station transmit power	43 dBm	Background noise	-100 dBm
Power of neighbor cell	37 dBm	Propagation models	Cost 231
Common channel power	30 dBm	COI's	CQI 1-6

In F2R2M, two fitness landscapes  $L_{hy}$  and  $L_{in}$  are defined by neighborhood functions  $\delta_H$  and  $\delta_I$ . In this paper, we focus on the following properties of a fitness landscape: 1) the distribution of feasible solutions within the search space; 2) the distribution of fitness space; and 3) the links between the distance and the solution fitnesses. To perform these analysis, two populations of solutions  $S_{ini}$  and  $S_{lo}$  are required.  $S_{ini}$  is composed of 600 initial solutions randomly chosen from solution space.  $S_{lo}$  is the population of local optima solutions found by applying hill climbing (HC) to  $S_{ini}$ . From solution  $x$ , HC evaluates all the feasible neighbors of  $x$  and replaces  $x$  by the neighbor which has the best fitness. HC stops when all neighbors are worse than  $x$ .

#### A. Analysis of Search Space

To study the distribution of feasible solutions in each space, we define two kinds of distance:  $d_{ini}$  and  $d_{lo}$  are the distances among any two solutions in  $S_{ini}$  and  $S_{lo}$ , respectively. Tables II(b) and II(a) present the minimum, the maximum and the median values (first and third quartile are also given) of these distances.

TABLE II  
ANALYSIS OF SEARCH SPACE: SOLUTION DISTANCE

(a) Distance between solutions of $L_{in}$						
Scen.	$d_{ini}$ in $S_{ini,in}$			$d_{lo}$ in $S_{lo,in}$		
	Min	Med <sub>Q1,Q3</sub>	Max	Min	Med <sub>Q1,Q3</sub>	Max
scen.1	15	62 <sub>54,72</sub>	109	17	62 <sub>54,71</sub>	108
scen.2	20	64 <sub>55,74</sub>	114	20	65 <sub>55,75</sub>	117
scen.3	20	64 <sub>55,73</sub>	116	20	64 <sub>55,74</sub>	116
scen.4	26	66 <sub>56,76</sub>	148	20	66 <sub>56,76</sub>	148
scen.5	10	53 <sub>44,63</sub>	92	12	54 <sub>45,63</sub>	99
scen.6	21	64 <sub>55,73</sub>	130	19	65 <sub>55,76</sub>	180

(b) Distance between solutions of $L_{hy}$						
Scen.	$d_{ini}$ in $S_{lo,hy}$			$d_{lo}$ in $S_{lo,hy}$		
	Min	Med <sub>Q1,Q3</sub>	Max	Min	Med <sub>Q1,Q3</sub>	Max
scen.1	19	62 <sub>53,71</sub>	108	0	34 <sub>23,45</sub>	109
scen.2	23	64 <sub>54,73</sub>	121	0	33 <sub>22,46</sub>	127
scen.3	21	65 <sub>54,73</sub>	115	0	43 <sub>30,57</sub>	138
scen.4	20	64 <sub>55,73</sub>	116	0	35 <sub>24,49</sub>	156
scen.5	24	55 <sub>64,73</sub>	114	0	63 <sub>39,86</sub>	157
scen.6	21	64 <sub>55,73</sub>	129	0	38 <sub>23,56</sub>	194

The statistics of  $d_{ini}$  shows that the random initial solutions for both search spaces are homogeneous. But the space of

local optima are different for two landscapes. In  $S_{lo,hy}$ , the minimum value of 0 indicates that there are same local optima found from different initial solutions. While in  $S_{lo,in}$ , no local optima solution have the same value. The quartiles (median, Q1 and Q3) show the space of  $S_{lo,hy}$  is more concentrated than  $S_{lo,in}$ . Therefore, for the population of local optima,  $L_{hy}$  appears closer than  $L_{in}$ .

#### B. Analysis of Fitness Space

The fitness value represents the quality of a solution. Figure 4 shows the distribution of fitness values of  $S_{ini}$  and  $S_{lo}$  for 3s-100u-snn.

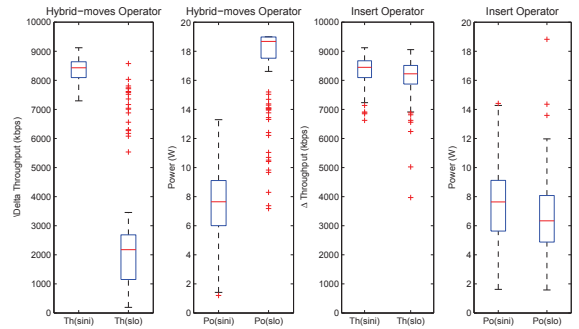


Fig. 4. Two fitness spaces of scenario 5 (3s-100u-snn)

We can observe that the fitness values of  $S_{ini}$  is well diversified, according to the similarity of the statistics in  $S_{ini}$  for all scenarios (Table II), we verify that the random initial populations are uniformly distributed. Then, all the fitness of local optima for both operators are better than the associated random initial solutions.

Moreover, in the first and third subfigures of Figure 4, the fitness of local optima for two operators are not flat, actually the quality of  $S_{lo,hy}$  is better than that of  $S_{lo,in}$  ( $Th_{hy} < Th_{in}$ ), the same situation for the other scenarios are shown in Table III, which shows the statistics of solution fitness of local optima in two landscapes, hence gives global information about the quality of  $S_{lo}$  determined by neighborhood operators. In Table III we can see  $\delta_H$  finds solutions with smaller  $Th(c)$ , hence better solutions than  $\delta_I$ . This can be explained by the fact that, unlike  $\delta_I$ ,  $\delta_H$  moves a block of elements which explores larger search space, so that it can easily escape from the local optimal.

#### C. Analysis of Links between Distance and Fitness

The step length is the number of moves from an initial solution to its associated local optima. In F2R2M, the step length is defined as the number of implemented operator applications by using hill climbing method.

Table IV presents the statistics of the step lengths to find local optima through  $\delta_H$  and  $\delta_I$ . Generally,  $\delta_I$  moves shorter distance than  $\delta_H$ , which may makes  $\delta_I$  walks nearby the initial solution without exploring to much better solution. Therefore,

TABLE III  
ANALYSIS OF FITNESS SPACE

(a) Fitness values of $S_{lo,in}$					
Scenarios		Min	Med <sub>Q1,Q3</sub>	Max	Mean
scen.1	Th(c) %	4.5	57.5 <sub>52.25,62</sub>	69	56.21
	Po(c) w	1.5	6.53 <sub>5.03,8.33</sub>	18.54	6.44
scen.2	Th(c) %	0	58.75 <sub>54,62</sub>	69.5	10.74
	Po(c) w	1.69	6.24 <sub>4.69,7.93</sub>	16.3	6.44
scen.3	Th(c) %	37	87.5 <sub>82,92</sub>	99	86.61
	Po(c) w	2.10	6.56 <sub>4.96,8.21</sub>	18.96	6.74
scen.4	Th(c) %	20.5	88 <sub>83.5,91.5</sub>	99	86.34
	Po(c) w	2.1	6.56 <sub>4.96,8.21</sub>	18.96	6.75
scen.5	Th(c) %	20.5	88 <sub>83.5,91.5</sub>	99	86.34
	Po(c) w	2.1	6.56 <sub>4.96,8.21</sub>	18.96	6.75
scen.6	Th(c) %	15.88	75.88 <sub>72.64,77.94</sub>	82.35	74.4
	Po(c) w	1.37	65.36 <sub>4.82,8.24</sub>	18.95	6.65

(b) Fitness values of $S_{lo,hy}$					
Scenarios		Min	Med <sub>Q1,Q3</sub>	Max	Mean
scen.1	Th(c) %	0	0 <sub>0,0</sub>	58	1.7
	Po(c) w	7.08	14.89 <sub>12.95,18.18</sub>	19.0	15.28
scen.2	Th(c) %	0	0 <sub>0,0</sub>	62.5	0.94
	Po(c) w	5.81	14.63 <sub>14.36,15.02</sub>	16.58	14.57
scen.3	Th(c) %	0	4 <sub>0,15</sub>	91.5	9.43
	Po(c) w	5.543	17.29 <sub>15.92,18.79</sub>	18.99	17.2
scen.4	Th(c) %	0	1 <sub>0,2</sub>	93.5	3.8
	Po(c) w	6.38	17.57 <sub>17.22,17.63</sub>	19.0	17.2
scen.5	Th(c) %	0	1 <sub>0,2</sub>	93.5	3.8
	Po(c) w	6.38	17.57 <sub>17.22,17.63</sub>	19.0	17.2
scen.6	Th(c) %	1.76	4.12 <sub>4.12,5.88</sub>	78.24	7.29
	Po(c) w	5.67	18.38 <sub>18.25,18.41</sub>	18.99	18.11

TABLE IV  
STEP LENGTHS OF TWO LANDSCAPES

Scen.	step length in $L_{in}$				step length in $L_{hy}$			
	Min	Med	Max	Mean	Min	Med	Max	Mean
scen.1	1	7	80	9.70	1	18	57	25.97
scen.2	1	7.5	126	10.74	1	21	62	26.93
scen.3	1	6	85	8.78	2	43	100	42.69
scen.4	1	7	127	11.1	1	61	114	67.61
scen.5	1	7	126	8.94	1	19.5	93	99.88
scen.6	1	11	181	12.62	5	105	166	99.88

$L_{in}$  seems “shallower” than  $L_{hy}$ , which explains that in Table II(a) the search space of  $S_{lo,in}$  does not concentrate the  $S_{ini,in}$ . Besides, local search with  $\delta_I$  may be faster, that is because the descent is deeper on landscape  $L_{hy}$ .

To investigate how the population of local optima is distributed in the search space relative to the optimum solution, we present fitness distance scatter plots of all scenarios (Figure 5 and Figure 6). These plots provide the fitness between local optima and the best found solution against their distances. The plots determine how closely the fitness and the distance related to the nearest optimum in the search space. When the distance to the best found solution becomes smaller, if fitness difference is decreased, then search procedure is expected to be easy to explored.

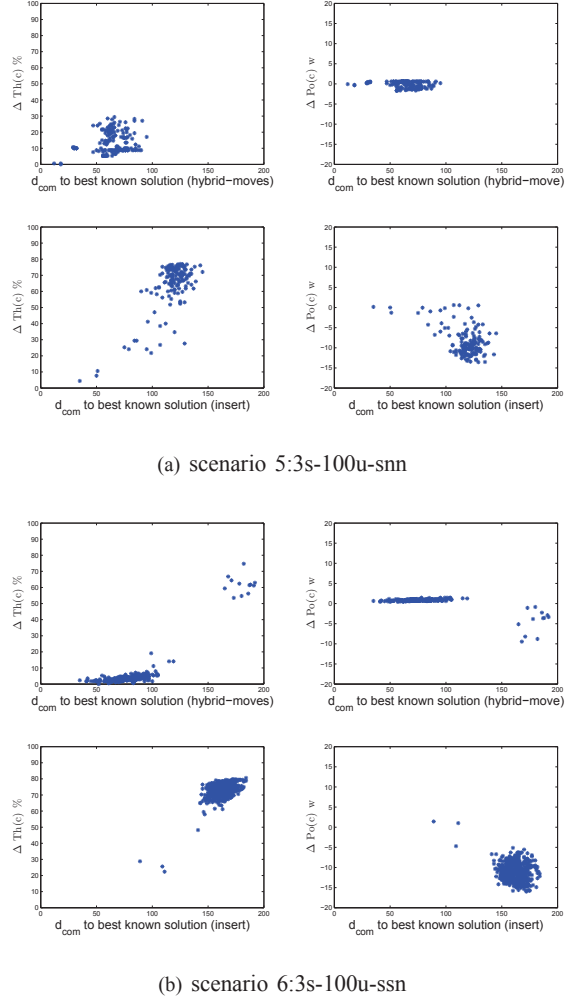


Fig. 5. Fitness-distance plots with local optima

Figure 5 reveals that all local optima are converged on a small region of the search space. The local optima found by  $\delta_H$  are more closer to the found best solution than the local optima found by  $\delta_I$ . When points locate in the different distance from the best found solution, their fitness difference are varied, that means both search space are rugged. But in the search space of  $\delta_I$ , the fitness and the distance to the best found solution is less correlated than in the search space of  $\delta_H$ . The same situation appears for the other instances (Figure 6), hence the problem difficulty with  $L_{in}$  is harder than  $L_{hy}$ . Meanwhile, scenarios 1, 2 (Figure 6(a) and Figure 6(b)) have higher correlation than in scenarios 5 and 6, that indicates the difficulty of search space is increased with the increasing scenario complexity.

The study of fitness landscape reveals that local optima in  $L_{hy}$  are closer to each other than in  $L_{in}$ , and that  $\delta_H$  can explore larger neighborhood space to achieve better solution than  $\delta_I$ . Therefore  $L_{hy}$  outperforms  $L_{in}$ .

#### IV. COMPARISON RESULTS

To prove the influence of landscape on optimization performance, 500 trails of greedy local search is implemented for two neighborhood operators on F2R2M.

TABLE V  
COMPARISON RESULTS WITH CONVENTIONAL APPROACHES

	MPC	DTM	S-FACH	S-MPC	F2R2M-in	F2R2M-hy
scen.1	0%	0%	65% 10.23	28% 21.51	4.5% 18.5	0% 10.19
scen.2	27.19	30.45	47% 15.4	16% 18.4	0% 15.58	0% 13.06
scen.3	0%	0%	25.4% 26.95	44.6% 21.51	25.4% 16.9	0% 15.0
scen.4	32.47	37.68	36.2% 22.63	47.4% 18.37	15.4% 16.5	0% 14.4
scen.5	0%	0%	59.41% 5.95	0% 31.1	36.47% 18.82	1.76% 18.39
scen.6	37.73	37.69	51.18% 15.9	0% 31.79	15.9% 18.12	1.76% 17.5

*two-dimensional cost: lost throughput in percentage, power consumption in watts*

The found best solutions of our model are shown in Table V. Competing allocation approaches are implemented on the same platform. To prove the advantage of layer based channel allocation, we applied MPC for each flow (S-MPC). We can observe that when services are transmitted in non-scalable mode, neither MPC nor DTM can obtain feasible solutions. S-FACH solves the power saturation problem of MPC and DTM for three scenarios. It reduces the coverage for the advanced flows hence consuming less power and provides service coverage (all service can be transmitted). However, in S-FACH, the trade-off between service quality and power is not efficient with fixed coverages. When most users are far from the base station (e.g.  $3s-80u$ ), S-FACH achieves power saturation.

The result of S-MPC shows that scalable transmission costs less power than non-scalable scheme thus has higher possibility to obtain feasible solution. From the results of S-MPC for  $2s-50u-sn/ss$  or  $3s-80u-snn/ssn$ , with the same user distribution and total traffic load, the scalable transmission of  $s2$  consumes less power. However, for scenarios having more users ( $3s-100u$ ), S-MPC increases the possibility of power saturation because it allocates only pure transmission mode per flow.

The F2R2M with local search outperforms the other algorithms. For the scenario that could obtain proper solutions with the conventional algorithms, F2R2M avoids unneeded QoS decrease. F2R2M-in with greedy local search can find feasible solutions, hence balance the consumption between power and channel codes. However, for scenario with increased complexity, its solution quality is reduced since  $Th(x)$  is higher. While F2R2M-hy found the best solution among all approaches, it always obtain feasible solution with much less  $Po(x)$  and almost achieve 100% bandwidth requirement.

The statistics of fitness values of found solutions are computed in Table VI, which proves the feasibility of all solutions

TABLE VI  
PERFORMANCE OF LOCAL SEARCH WITH  $\delta_I$  AND  $\delta_H$

Scen.	F2R2M-in			F2R2M-hy		
	best	mean	std.	best	mena	std.
scen.1	4.5% 18.5	56.2% 6.4	8.12 8.12	0% 10.19	1.7% 15.28	8.18 2.56
scen.2	0% 15.58	57.29% 6.44	7.82 2.27	0% 13.06	0.94% 14.57	6.46 0.9
scen.3	25.4% 16.9	66.62% 6.73	5.53 2.29	0% 15	7.25% 17.12	11.77 2.0
scen.4	15.4% 16.5	66.42% 6.75	6.73 2.45	0% 14.4	2.9% 17.2	11.26 1.23
scen.5	36.47% 18.82	74.98% 6.58	4.5337 2.3244	1.76% 18.39	19.57% 18.03	12.61 1.5856
scen.6	15.9% 18.12	74.4% 6.65	7.13 2.55	1.76% 17.5	7.29% 18.12	11.93 1.4

obtained with F2R2M.  $\delta_H$  can always offer good enough solutions: higher QoS with less power consumption than the competing approaches. Besides, the performance of  $\delta_H$  is better than  $\delta_I$ , which proves the discussion in section III that  $\delta_H$  has capacity of “jump” from local optima, while  $\delta_I$  can only stay in basins. In Table VII, the average consuming time of search procedure for two operators are both acceptable,  $\delta_H$  costs almost double time than  $\delta_I$ , that is because  $\delta_H$  can move further than  $\delta_I$ .

TABLE VII  
AVERAGE TIME COST (S) OF F2R2M

Scen.	F2R2M-in	F2R2M-hy	Scen.	F2R2M-in	F2R2M-hy
scen.1	0.062	0.160	scen.2	0.122	0.259
scen.3	0.18	0.322	scen.4	0.117	0.279
scen.5	0.196	0.368	scen.6	0.313	0.773

#### V. CONCLUSION AND PERSPECTIVE

In this paper, we present a mathematical model which enables flexible radio resource allocation for simultaneous MBMS services. This model integrates scalable transmissions and dynamic power setting along with transmit mode selection. The proposed evaluation criterion guides the search to satisfy two objects in a lexicographic order: first to achieve the QoS requirement of multicast service and then to minimize the power consumption.

In order to understand the problem behavior differentiated by the proposed two neighborhood functions, we developed the mathematic solution representation and the distance measurement between two feasible solutions, based on which, the fitness landscapes analysis is conducted. The fitness distance plot shows both search space are rugged, and the  $\delta_H$  is more powerful than  $\delta_I$  in terms of escaping from the local optima. Following by that, simulations are carried out in a variety of scenarios. Both operators in our model are capable of producing high quality solutions with a preferable balance

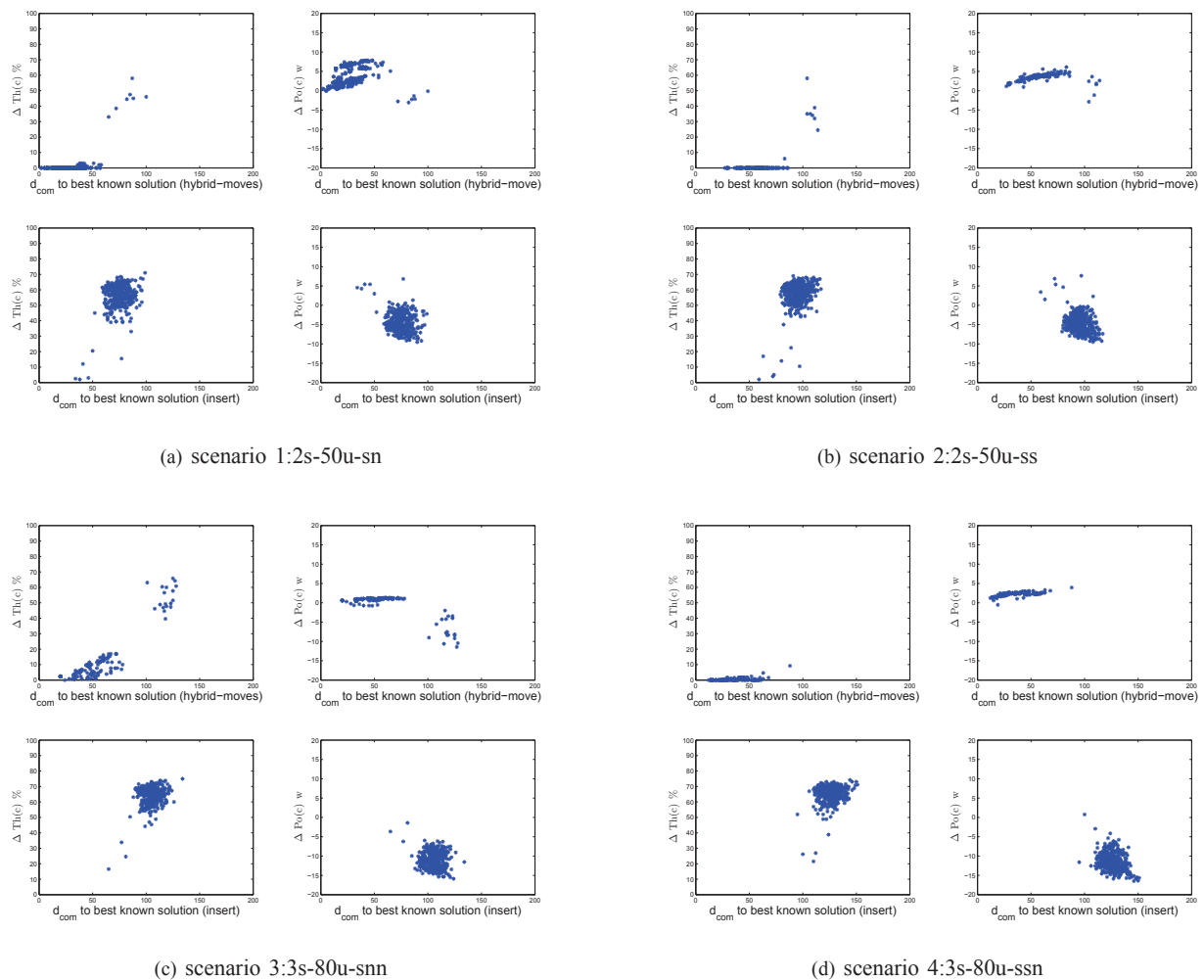


Fig. 6. Fitness-distance plots with local optima

between radio resource consumption, service coverage and service quality. In particular, the hybrid-moves operator is able to find near-optimum solutions in all scenarios.

However, robustness against local optima still has to be improved in our search algorithms. In other words, the greedy local search method does not always reach the theoretical best found solution in every trial. That is because that the algorithm terminates when it reaches a state where no further improvement can be found. In the future work, we are interested in applying the effective metaheuristics capable of escaping from local optima (e.g. simulated annealing and Tabu search) to our model to obtain solutions with higher stability.

#### REFERENCES

- [1] 3GPP TS 25.213 Spreading and modulation (FDD).
- [2] 3rd Generation Partnership Project R1-021240 TSG-RAN WG128 Power Usage for Mixed FACH and DCH for MBMS, 2002.
- [3] 3GPP TR 25.803 S-CCPCH performance for MBMS, September 2005.
- [4] 3GPP TS 25.214 Physical layer procedures (FDD), June 2005.
- [5] 3GPP TR 25.922 radio resource management strategies, March 2007.
- [6] 3GPP TS 23.246 multimedia broadcast/multicast service (mbms); architecture and functional description (release 6), June 2007.
- [7] A. Alexiou, C. Bouras, and E. Rekkas. A power control scheme for efficient radio bearer selection in MBMS. In *World of Wireless, Mobile and Multimedia Networks, 2007. WoWMoM 2007. IEEE International Symposium on a*, pages 1–8, June 2007.
- [8] C. Christophorou, A. Pitsillides, and T. Lundborg. Enhanced radio resource management algorithms for efficient mbms service provision in UTRAN. *Computer Networks*, 55(3):689–710, 2011.
- [9] A. M. C. Correia, J. C. M. Silva, N. M. B. Souto, L. A. C. Silva, A. B. Boal, and A. B. Soares. Multi-resolution broadcast/multicast systems for MBMS. *Broadcasting, IEEE Transactions on*, 53(1):224–234, March 2007.
- [10] P. Czerepinski, T. Chapman, and J. Krause. Coverage and planning aspects of MBMS in UTRAN. In *Fifth IEE International Conference on 3G Mobile Communication Technologies, 2004. 3G 2004*, 2004.
- [11] J. C. S. n. S. F. C. A. C. Frank Brouwer, irene de Bruin, editor. *Usage of link-level performance indicators for HSDPA network-level simulations in E-UMTS*. Proceedings of IEEE ISSSTA 04, 2004.
- [12] A. T. Harri Holma. *HSDPA/HSUPA for UMTS: High Speed Radio Access for Mobile Communications*. John Wiley & Sons, 2006.
- [13] J. P. Romero, O. Sallent, R. Agusti, and M. A. Diaz-Guerra. *Radio Resource Management Strategies in UMTS*. Wiley, 1 edition, Aug. 2005.
- [14] P. F. Stadler. *Towards a Theory of Landscapes*. 1995.
- [15] Wright. The roles of mutation, inbreeding, crossbreeding and selection in evolution. *Proceedings of the Sixth International Congress of Genetics*, 1:35666, 1932.